and 10^{-1} s on the (100) facet. Therefore, the ability of the surfactant ligands to move on the surface allows the (111) facet to grow, whereas the low mobility of the ligands on the (100) facet blocks its growth. However, this mechanism is only for large facets. For small nanocrystals, the ligand molecules can easily fan out to make room for platinum atoms to land (*14*). Therefore, all facets grow when the nanocrystal is small. The critical size of about 5 nm may vary with temperature or the type of ligand. Our proposed ligand mobility–controlled selective facet–arrested shape evolution may apply to other ligands and nanoparticle shapes.

REFERENCES AND NOTES

1. C. J. Murphy *et al.*, *J. Phys. Chem. B* **109**, 13857–13870 (2005).
2. Z. Tang, N. A. Kotov, M. Giersig, *Science* **297**, 237–240 (2002).
3. C. Burda, X. Chen, R. Narayanan, M. A. El-Sayed, *Chem. Rev.* **105**, 1025–1102 (2005).
4. M. Bruchez Jr., M. Moronne, P. Gin, S. Weiss, A. P. Alivisatos, *Science* **281**, 2013–2016 (1998).
5. M. C. Daniel, D. Astruc, *Chem. Rev.* **104**, 293–346 (2004).
6. R. Elghanian, J. J. Storhoff, R. C. Mucic, R. L. Letsinger, C. A. Mirkin, *Science* **277**, 1078–1081 (1997).
7. P. L. Hansen *et al.*, *Science* **295**, 2053–2055 (2002).
8. E. Ringe, R. P. Van Duyne, L. D. Marks, *Nano Lett.* **11**, 3399–3403 (2011).
9. J. W. Gibbs, H. A. Bumstead, R. G. Van Name, W. R. Longley, *The Collected Works of J. Willard Gibbs* (Longmans, Green, City, 1902).
10. G. Wulff, *Z. Kristallogr. Mineral.* **34**, 449–530 (1901).
11. N. Tian, Z.-Y. Zhou, S.-G. Sun, Y. Ding, Z. L. Wang, *Science* **316**, 732–735 (2007).
12. Y. Xia, Y. Xiong, B. Lim, S. E. Skrabalak, *Angew. Chem. Int. Ed.* **48**, 60–103 (2009).
13. A. R. Tao, S. Habas, P. Yang, *Small* **4**, 310–325 (2008).
14. C. R. Bealing, W. J. Baumgardner, J. J. Choi, T. Hanrath, R. G. Hennig, *ACS Nano* **6**, 2118–2127 (2012).
15. M. J. Williamson, R. M. Tromp, P. M. Vereecken, R. Hull, F. M. Ross, *Nat. Mater.* **2**, 532–536 (2003).
16. H. Zheng *et al.*, *Science* **324**, 1309–1312 (2009).
17. J. E. Evans, K. L. Jungjohann, N. D. Browning, I. Arslan, *Nano Lett.* **11**, 2809–2813 (2011).
18. N. de Jonge, F. M. Ross, *Nat. Nanotechnol.* **6**, 695–704 (2011).
19. J. M. Yuk *et al.*, *Science* **336**, 61–64 (2012).
20. Y. Borodko *et al.*, *J. Phys. Chem. C* **117**, 26667–26674 (2013).
21. H.-G. Liao, L. Cui, S. Whitelam, H. Zheng, *Science* **336**, 1011–1014 (2012).

ACKNOWLEDGMENTS

We thank B. Sadtler for useful comments on the manuscript. Part of the in situ experiments was performed at Gatan, Incorporated using a Tecnai equipped with a K2-IS camera. We also used FEI Titan, Tecnai UT20, JOEL3010, and TEAM0.5 microscopes at the National Center for Electron Microscopy of Lawrence Berkeley National Laboratory, which is supported by the U.S. Department of Energy (DOE) Office of Basic Energy Sciences under contract no. DE-AC02-05CH11231. H.Z. was a residency faculty member of SinBeRise program of BEARS at University of California, Berkeley, during July 2013 to January 2014 and thanks the DOE Office of Science Early Career Research Program for support.

SUPPLEMENTARY MATERIALS

www.sciencemag.org/content/345/6199/916/suppl/DC1
Materials and Methods
Supplementary Text
Figs. S1 to S20
References (*22*–*32*)
Movies S1 to S7

10 March 2014; accepted 3 July 2014
10.1126/science.1253149

GLACIERS

Attribution of global glacier mass loss to anthropogenic and natural causes

Ben Marzeion,[1]* J. Graham Cogley,[2] Kristin Richter,[1] David Parkes[1]

The ongoing global glacier retreat is affecting human societies by causing sea-level rise, changing seasonal water availability, and increasing geohazards. Melting glaciers are an icon of anthropogenic climate change. However, glacier response times are typically decades or longer, which implies that the present-day glacier retreat is a mixed response to past and current natural climate variability and current anthropogenic forcing. Here we show that only 25 ± 35% of the global glacier mass loss during the period from 1851 to 2010 is attributable to anthropogenic causes. Nevertheless, the anthropogenic signal is detectable with high confidence in glacier mass balance observations during 1991 to 2010, and the anthropogenic fraction of global glacier mass loss during that period has increased to 69 ± 24%.

Although glaciers store less than 1% of global ice mass (*1*), their mass loss has been a major cause of sea-level rise during the 20th century (*2*). Glaciers are important regulators of the seasonal water cycle, providing meltwater during dry seasons in many regions of the world (*3*, *4*). Glacier retreat often leads to the destabilization of mountain slopes and the formation of unstably dammed meltwater lakes, increasing the risk of rockslides and catastrophic outburst floods (*5*). The worldwide retreat of glaciers over the past decades has therefore had many impacts on human societies, which should increase over the 21st century because of continued mass losses (*6*–*8*).

Even though warming has accelerated over recent decades (*9*), glaciers have contributed to sea-level rise during most of the 20th century with relatively constant mass loss rates (*2*, *6*, *10*). The mass loss during the first decades of the 20th century was presumably governed by the loss of ice at low altitudes, when glaciers retreated from their 19th-century maxima at the end of the Little Ice Age (*11*). Because glacier extent responds to changes in the glacier mass balance (MB) with a lag of decades to centuries (*12*–*14*), glaciers provide an opportunity to directly perceive long-term climate change, unobscured by interannual variability. For this reason, images of retreating glaciers have become widely publicized illustrations of anthropogenic climate change. At the same time, the lagged response of glacier extents to climate changes complicates the attribution of the observed changes to any particular cause, because glacier mass change at any time is in part an ongoing adjustment of the glacier to previous climate change. The global retreat of glaciers observed today started around the middle of the 19th century, coinciding with the end of the Little Ice Age (*10*), when the anthropogenic forcing of the climate system was very weak as compared to today (*15*). Given the response times of glaciers, it is therefore reasonable to hypothesize that glaciers at present are responding both to naturally caused climate change of past centuries and to the anthropogenic warming that has become stronger in recent decades. There is evidence that the recent mass loss of individual glaciers exceeds values expected from internal variability (*16*), and a rough estimate has been made of the influence of anthropogenic warming on global glacier mass loss (*17*), but the explicit attribution of observed changes of individual glaciers is also complicated by the dynamic response of glaciers' geometries to climate forcing, because internal variability alone may cause glacier changes of the magnitude observed since the end of the Little Ice Age (*18*).

Here we quantify the evidence for a causal link between anthropogenic climate forcing and observed glacier surface MBs, not of individual glaciers but of all the world's glaciers outside of Antarctica combined. We then attribute the global glacier retreat since 1851 to natural and anthropogenic causes. We use a model of global glacier evolution that treats the MB of each of the world's glaciers contained in the Randolph Glacier Inventory (RGI) (*19*, *20*) individually, including a simple parametrization of ice dynamics leading to glacier hypsometry change (*6*). Forced by observed climate (*21*, *22*), the glacier model has been independently validated against both annual surface MB observations (fig. S1) and observed, temporally accumulated volume changes of hundreds of glaciers (*23*), and has been used to reconstruct and project the global glacier mass change from 1851 to 2300 (*6*), based on climate reconstructions and projections from the Coupled Model Intercomparison Project phase 5 (CMIP5). See the supplementary materials for a comprehensive description of the model.

For each of 12 reconstructions of the global climate between 1851 and 2010, produced by general circulation models (GCMs) from the CMIP5 ensemble (see table S1 for the list of the experiments used), we reconstructed the area and volume of each glacier in 1851 (*6*). From this

[1]Institute of Meteorology and Geophysics, University of Innsbruck, Austria. [2]Department of Geography, Trent University, Peterborough, Canada.
*Corresponding author. E-mail: ben.marzeion@uibk.ac.at

reconstructed glacier state, we modeled the evolution of each glacier forward in time. This forward model was run twice for each GCM: once subject to all known forcings (i.e., solar variability, volcanic eruptions, land-use change, anthropogenic aerosols, and greenhouse gas emissions; we call these model runs the FULL runs below), and once subject to only natural forcings (i.e., solar variability and volcanic eruptions; we call these model runs the NAT runs below). Figure 1A shows the ensemble mean and standard deviation of the global mean specific MBs for the FULL and NAT runs. Because the global mean specific MB interpolated from observations (*23*) (we call these OBS below) is available as pentadal means only (black lines in Fig. 1A), we determined the pentadal means of the model runs (thick solid lines in Fig. 1A). In order to determine whether the modeled glacier MBs are consistent with observed MBs, we calculated the confidence level of the difference between modeled and observed MBs for each pentad. High confidence in this difference (i.e., red shading in Fig. 1B) thus indicates model results that are inconsistent with observations.

Modeled MBs in both the FULL and NAT runs are negative over essentially the entire period considered. However, a difference emerges over the course of the 20th century: Although the MB of the NAT runs becomes less negative as glaciers retreat to higher altitudes, thus stabilizing their MBs, there is a clear trend toward more negative MBs of glaciers in the FULL runs after 1965. Modeled MBs in the FULL runs are generally consistent with observations during the entire period covered by the latter, whereas the NAT runs are inconsistent with observations for at least the four pentads spanning 1991 to 2010 (Fig. 1B). This means that the anthropogenic signal is detectable in observed MBs over these four pentads with high confidence, unaffected by the result that MBs would have been negative during this period even without anthropogenic climate forcing. The anthropogenic fraction of global specific glacier mass loss rates increased from $-6 \pm 35\%$ during the period 1851 to 1870 to $69 \pm 24\%$ during the period 1991 to 2010 (Fig. 1C, uncertainties correspond to one ensemble standard deviation). Without anthropogenic influence, glaciers would have contributed 99 ± 36 mm to global mean sea-level rise during 1851 to 2010. With anthropogenic influence, this number increases to 133 ± 30 mm (Fig. 1D, uncertainties correspond to one ensemble standard deviation).

When global mean MBs over longer periods than pentads are considered, it becomes evident that the NAT runs are inconsistent with observations for any period spanning 5 to 50 years and ending in 2010 (Fig. 2). The FULL runs are generally consistent with observations (Fig. 1B), but the simulated MBs are more negative than the observations during 2001 to 2010 (Fig. 1A), resulting in a difference between FULL runs and observations above the 85% confidence level for periods spanning 5 to 15 years and ending in 2010 (Fig. 2). This difference is caused by the FULL MBs for Svalbard and the Russian Arctic, which are too negative as compared to the observations.

Glacier mass losses attributable to human activity (shown as a fraction in Fig. 1C) have increased nearly steadily since 1860. In Fig. 3 we plot the year-by-year anthropogenic global mean specific mass balance $MB_{ANTH} = MB_{FULL} - MB_{NAT}$ against the concurrent anthropogenic radiative forcing R (*24*), and find a sensitivity dMB_{ANTH}/dR of -209 ± 33 kg year^{-1} W^{-1} (uncertainty corresponds to the 95% confidence interval). This is about twice as much as a direct calculation based on the latent heat of fusion of ice would give (-94 kg year^{-1} W^{-1}), indicating that feedbacks and the spatial distribution of anthropogenic climate change play an important role.

On the regional scale, the increased signal from internal climate variability, and greater uncertainty of GCM results (*25*), reduce the detectability of the anthropogenic signal. Although there are some regions where the anthropogenic signal is detectable (i.e., FULL runs are consistent with observations, whereas NAT runs are inconsistent), there are also a number of regions where the FULL runs are not consistent with observations (Fig. 2). The anthropogenic signal is detectable with high confidence in Alaska, western Canada and United States, Arctic Canada north and south, Greenland (only peripheral glaciers and not the ice sheet are considered there), north Asia, central Europe, low latitudes, and New Zealand (9 out of 18 regions), and with lesser confidence in Iceland, Scandinavia, and central Asia north (3 out of 18 regions). In Svalbard, the Russian Arctic, the Caucasus and Middle East, and the southern Andes, the FULL runs are inconsistent with observations (4 out of 18 regions), and in central Asia south and west both FULL and NAT runs are consistent with observations (2 out of 18 regions). A closer look at those regions where our method fails reveals that in the Caucasus and Middle East and the southern Andes, both the FULL and NAT runs underestimate the mass losses (in both cases, the FULL runs are closer to observations than the NAT runs).

In Svalbard and the Russian Arctic, the FULL run overestimates the mass loss, whereas the

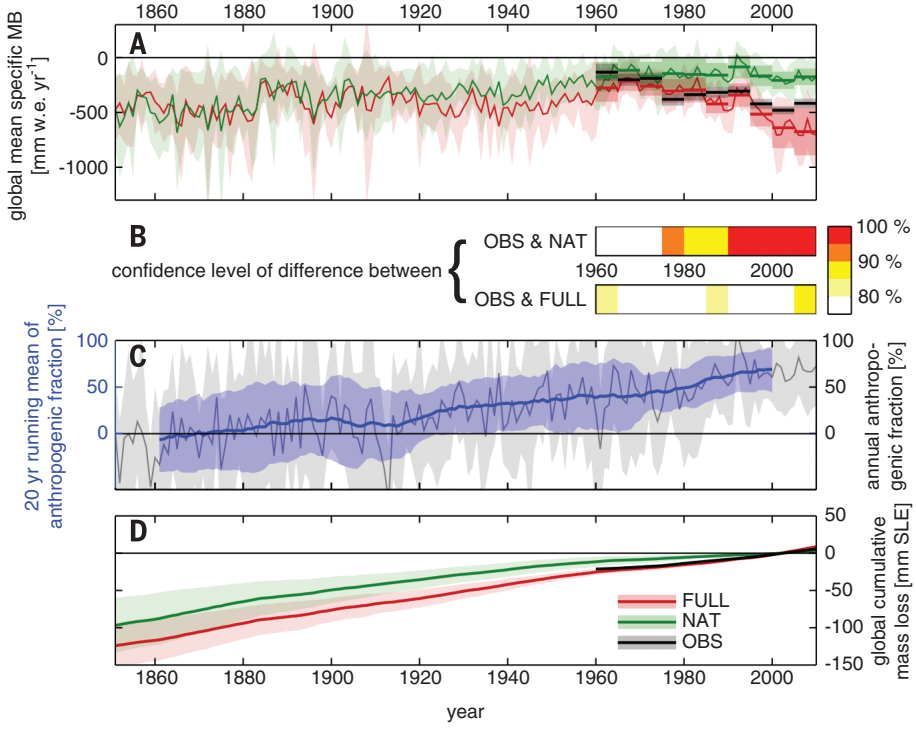

Fig. 1. Attribution of the anthropogenic signal in global mean glacier MBs. (**A**) Global mean specific MB time series (thin lines are the ensemble means, shading indicates one ensemble standard deviation) and pentadal means (thick lines are the ensemble means, shading indicates 1 SE; see the supplementary materials for the derivation of the error) are shown. Green, NAT results; red, FULL results; black, observations. (**B**) Confidence level of the difference between interpolated observations (OBS) updated from Cogley (2009) (*23*) and model results for the NAT and FULL models for each pentad. (**C**) Anthropogenic fraction of total glacier mass loss, annual values (gray), and running mean over 20-year periods (blue); the solid line is the ensemble mean; shading indicates one ensemble standard deviation. (**D**) Glacier contribution to global mean sea-level rise, relative to the mean of 1991 to 2010. Modeled results include modeled glacier area change; observations assume constant glacier area, as in the RGI (*19*) (the solid lines are the ensemble means; shading indicates one ensemble standard deviation).

NAT run is consistent with observations (fig. S2). GCMs tend to have greater errors in this region than on global average (*25*), but they do not generally exhibit a stronger warming during summer months or reduced precipitation as compared to observations (*22*), which could explain too-negative modeled MBs. When we exclude calving glaciers from the observational data set (calving is not accounted for in the glacier model but does affect the observational estimate), the difference is reduced slightly, but not enough to lead to consistent results in these regions. Because validation of the glacier model on individual glaciers, as opposed to the regional mean, does not indicate a general underestimation of the modeled MBs in Svalbard (*6*), the reason for this regional inconsistency has to be related to the sampling of glacier MB observations (*26*), but ultimately remains unclear.

Because the glaciers are considerably out of balance with both modeled FULL and NAT climate at the beginning of the simulation period, it is not possible to distinguish between glacier mass losses caused by internal variability and natural forcing. In order to address this question, it would be necessary to identify the causes that led to the buildup of glacier mass during the Little Ice Age, a period not covered by the CMIP5 experiments. However, our results indicate that a considerable fraction of 20th-century glacier mass loss, and therefore also of observed sea-level rise, was independent of anthropogenic climate forcing. At the same time, we find unambiguous evidence of anthropogenic glacier mass loss in recent decades.

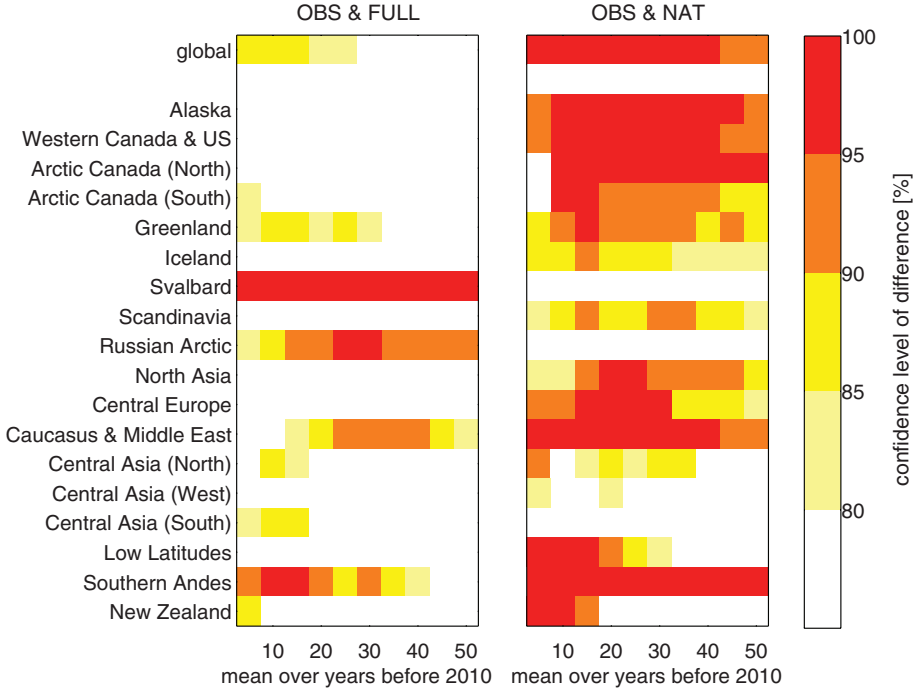

Fig. 2. Detection of the anthropogenic signal in global and regional glacier MBs over longer time intervals. Confidence levels of difference between observations (*23*) and model results for the NAT and FULL models for periods of different length ending in 2010 are shown. Regions are as defined in the RGI (*19*).

Fig. 3. Sensitivity of the instantaneous anthropogenic global mean specific MB to global mean anthropogenic radiative forcing. Annual values of MB_{ANTH} plotted against concurrent anthropogenic radiative forcing *R* (*24*) are shown. The Pearson correlation coefficient between the two is −0.71.

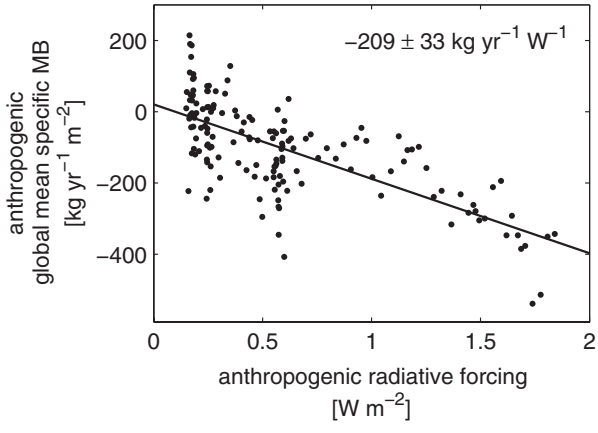

REFERENCES AND NOTES

1. D. G. Vaughan *et al.*, in *Climate Change 2013: The Physical Science Basis. Contribution of Working Group I to the Fifth Assessment Report of the Intergovernmental Panel on Climate Change*, T. F. Stocker, D. Qin, G.-K. Plattner, M. Tignor, S. K. Allen, J. Boschung, A. Nauels, Y. Xia, V. Bex, P. M. Midgley, Eds. (Cambridge Univ. Press, Cambridge, 2013), pp. 317–382.
2. J. M. Gregory *et al.*, *J. Clim.* **26**, 4476–4499 (2013).
3. W. W. Immerzeel, L. P. H. van Beek, M. F. P. Bierkens, *Science* **328**, 1382–1385 (2010).
4. G. Kaser, M. Grosshauser, B. Marzeion, *Proc. Natl. Acad. Sci. U.S.A.* **107**, 20223–20227 (2010).
5. S. D. Richardson, J. M. Reynolds, *Quat. Int.* **65-66**, 31–47 (2000).
6. B. Marzeion, A. H. Jarosch, M. Hofer, *Cryosphere* **6**, 1295–1322 (2012).
7. R. H. Giesen, J. Oerlemans, *Clim. Dyn.* **41**, 3283–3300 (2013).
8. V. Radić *et al.*, *Clim. Dyn.* **42**, 37–58 (2014).
9. D. L. Hartmann *et al.*, in *Climate Change 2013: The Physical Science Basis. Contribution of Working Group I to the Fifth Assessment Report of the Intergovernmental Panel on Climate Change*, T. F. Stocker, D. Qin, G.-K. Plattner, M. Tignor, S. K. Allen, J. Boschung, A. Nauels, Y. Xia, V. Bex, P. M. Midgley, Eds. (Cambridge Univ. Press, Cambridge, 2013), pp. 159–254.
10. P. W. Leclercq, J. Oerlemans, J. G. Cogley, *Surv. Geophys.* **32**, 519–535 (2011).
11. B. Marzeion, A. H. Jarosch, J. M. Gregory, *Cryosphere* **8**, 59–71 (2014).
12. T. Jóhannesson, C. Raymond, E. Waddington, *J. Glaciol.* **35**, 355–369 (1989).
13. W. Harrison, D. Elsberg, K. Echelmeyer, R. Krimmel, *J. Glaciol.* **47**, 659–664 (2001).
14. J. Oerlemans, *Science* **308**, 675–677 (2005).
15. G. Myhre *et al.*, in *Climate Change 2013: The Physical Science Basis. Contribution of Working Group I to the Fifth Assessment Report of the Intergovernmental Panel on Climate Change*, T. F. Stocker, D. Qin, G.-K. Plattner, M. Tignor, S. K. Allen, J. Boschung, A. Nauels, Y. Xia, V. Bex, P. M. Midgley, Eds. (Cambridge Univ. Press, Cambridge, 2013), pp. 659–740.
16. B. K. Reichert, L. Bengtsson, J. Oerlemans, *J. Clim.* **15**, 3069–3081 (2002).
17. J. Oerlemans, *J. Glaciol.* **34**, 333–341 (1988).
18. G. Roe, M. O'Neal, *J. Glaciol.* **55**, 839–854 (2009).
19. A. Arendt *et al.*, *Randolph Glacier Inventory 1.0: A Dataset of Global Glacier Outlines* (Global Land Ice Measurements from Space, Boulder, CO, 2012), digital media.
20. W. T. Pfeffer *et al.*, *J. Glaciol.* **60**, 537–552 (2014).
21. M. New, D. Lister, M. Hulme, I. Makin, *Clim. Res.* **21**, 1–25 (2002).
22. T. D. Mitchell, P. D. Jones, *Int. J. Climatol.* **25**, 693–712 (2005).
23. J. G. Cogley, *Ann. Glaciol.* **50** (50), 96–100 (2009).
24. M. Meinshausen *et al.*, *Clim. Change* **109**, 213–241 (2011).
25. G. Flato *et al.*, in *Climate Change 2013: The Physical Science Basis. Contribution of Working Group I to the Fifth Assessment Report of the Intergovernmental Panel on Climate Change*, T. F. Stocker, D. Qin, G.-K. Plattner, M. Tignor, S. K. Allen, J. Boschung, A. Nauels, Y. Xia, V. Bex, P. M. Midgley, Eds. (Cambridge Univ. Press, Cambridge, 2013), pp. 741–866.
26. A. S. Gardner *et al.*, *Science* **340**, 852–857 (2013).

ACKNOWLEDGMENTS

This work was funded by the Austrian Science Fund (grant PP25362-N26) and supported by the Austrian Ministry of Science Bundesministerium für Wissenschaft und Forschung as part of the UniInfrastrukturprogramm of the Research Platform Scientific Computing at the University of Innsbruck. We acknowledge the World Climate Research Programme's Working Group on Coupled Modelling, which is responsible for CMIP, and we thank the climate modeling groups (listed in the table S1) for producing and making available their model output. For CMIP, the U.S. Department of Energy's Program for Climate Model Diagnosis and Intercomparison provided coordinating support and led the development of software infrastructure in partnership with the Global Organization for Earth System Science Portals.

SUPPLEMENTARY MATERIALS

www.sciencemag.org/content/345/6199/919/suppl/DC1
Methods
Figs. S1 and S2
Table S1
References (*27*–*33*)

11 April 2014; accepted 14 July 2014
10.1126/science.1254702